

## Isolation and Characterization of Bacterial Nucleoids in Microfluidic Devices

James Pelletier and Suckjoon Jun

### Abstract

We report methods for isolation of *Escherichia coli* nucleoids in microfluidic devices, allowing characterization of nucleoids during a controlled in vivo to in vitro transition. Biochemically, nucleoids are isolated by gentle osmotic lysis, which minimally perturbs nucleoid-associated proteins (NAPs). Biophysically, nucleoids are isolated in microfluidic chambers, which mimic confinement within the cell, as well as facilitate diffusive buffer exchange around nucleoids without subjecting them to flow. These methods can be used to characterize interactions between NAPs and whole nucleoids, and to investigate nucleoid structure and dynamics in confinement. We present protocols for isolation, quantification, and perturbation of nucleoids in microfluidic confinement.

**Key words** Nucleoid isolation, Microfluidics, Nucleoid-associated proteins, Molecular crowding

---

### 1 Introduction

During the *Escherichia coli* cell cycle, physiological processes such as regulation of gene expression, and genome replication and segregation, depend on nucleoid structure and dynamics. How do nucleoid-associated proteins (NAPs) and confinement within the cell facilitate these complex functions? About ten known NAPs contribute to nucleoid organization and have a wide range of functions [1, 2]. Their abundances depend on the growth physiology and change from exponential to stationary phase [3]. Diverse experiments have elucidated how the nucleoid is influenced by NAPs and thermodynamic driving forces such as macromolecular crowding and conformational entropy.

In vitro approaches complement and facilitate measurements and perturbations not possible in vivo, but they often involve simplified DNA substrates and NAP mixtures. We developed a microfluidic device to isolate whole nucleoids in chambers, offering a bridge between in vivo and in vitro regimes [4]. The devices offer

control over the timing of lysis, allowing us to image the lysis process.

We adapted a gentle osmotic lysis method that minimally perturbs DNA–protein interactions and yields nucleoids free of cell envelope fragments [5]. Thus, the nucleoids begin with their full complement of NAPs at in vivo concentrations, at least an order of magnitude greater than typical in vitro concentrations.

After nucleoid isolation, the microfluidic devices offer biochemical and biophysical control over the nucleoids. The chambers enable rapid ambient buffer exchange via diffusion, without subjecting the nucleoids to flow. Furthermore, different micron-scale chamber geometries impose different degrees of confinement. We anticipate microfluidic nucleoid isolation will enable biochemical characterization of diverse NAPs as well as biophysical characterization of nucleoid structure and dynamics in confinement.

---

## 2 Materials

### 2.1 Microfluidics

- Polydimethylsiloxane (PDMS).
- Coring tool, such as 1.5 mm inner diameter, which is compatible with 1/16" outer diameter tubing.
- Glass coverslips.
- Plasma system, to bond PDMS to glass.
- Poly-L-lysine (20 kDa) grafted with polyethylene glycol (5 kDa) (SuSoS AG, PLL(20)-g[3.5]-PEG(5)).
- Syringe, such as 250  $\mu$ L Hamilton Gastight Luer tip.
- Luer to tubing adapter and fitting.
- Soft tubing, such as 0.01" ID, 1/16" OD HPFA+.
- Stiff tubing, such as 0.005" ID, 1/16" OD PEEK tubing.<sup>1</sup>
- Syringe pump.<sup>2</sup>
- Multiport selection valve.<sup>3</sup>

### 2.2 Buffers and Reagents

- Growth medium, such as Luria–Bertani (LB), stored at room temperature.<sup>4</sup>
- Sucrose buffer, stored at room temperature.  
20% sucrose (w/v).

---

<sup>1</sup> Stiffer tubing gives improved control over flows, for experiments in which the timing of buffer exchange is critical, such as nucleoid expansion after cell lysis.

<sup>2</sup> For experiments that require precise control of flow, we recommend a pressure-driven pump or hydrostatic pressure system [6].

<sup>3</sup> The valve facilitates buffer changes after nucleoid isolation.

<sup>4</sup> When physiology is important, we recommend optimized synthetic media.

100 mM NaCl.

10 mM NaPi, pH 7.3.

10 mM EDTA.

- Lysis buffer, stored at 4 °C.  
40–200 mM NaCl.  
20 mM Na-HEPES, pH 7.5.  
0.5 mg/mL bovine serum albumin (BSA).
- Lysozyme, from chicken egg white, stored at –20 °C.
- 0.1 mg/mL PLL-g-PEG in 10 mM Na-HEPES, pH 7.4. Store solution at 4 °C for up to 2 weeks.<sup>5</sup>
- Hoechst 33342, trihydrochloride, trihydrate, 100 mg (Thermo Fisher H1399), store powder at room temperature in dark. Prepare 10 mg/mL stock solution in water and store at 4 °C in dark.

---

## 3 Methods

### 3.1 *Microfluidic Device*

The microfluidic device (Fig. 1) facilitates gentle nucleoid isolation by osmotic shock then subsequent biochemical perturbation of the nucleoids, without subjecting the nucleoids to flow. In particular, nucleoids are isolated in microfluidic chambers. Like a cul-de-sac, each chamber opens on one end to a channel, whereas the other end is closed, so there is no flow through the chamber. Rather, buffer in the chambers exchanges with buffer in the channel via diffusion.

To investigate nucleoids in channel-like confinement, we used chambers shaped as rectangular prisms, 1.7  $\mu\text{m}$  wide  $\times$  1.5  $\mu\text{m}$  deep  $\times$  25  $\mu\text{m}$  long, just wide and deep enough to accommodate a single row of cells. Over that chamber length, diffusive buffer exchange happens in several seconds. Spaced 5  $\mu\text{m}$  apart, to decrease scattering of fluorescence between them, chambers are arranged perpendicular to a channel, 100  $\mu\text{m}$  wide  $\times$  30  $\mu\text{m}$  deep  $\times$  several cm long. The channel connects on one end to an inlet and on the other to an outlet. The devices are made of polydimethylsiloxane (PDMS) and a glass coverslip.

#### 3.1.1 *Microfluidic Master Fabrication*

Detailed microfluidic master fabrication protocols are available on the Jun lab website (<https://jun.ucsd.edu>). In contrast to the cell growth devices, which are treated with pentane then acetone to remove uncured PDMS toxic to cells, nucleoid devices are not treated, as any treatment can distort the chamber geometries.

---

<sup>5</sup> Static electricity causes the highly charged powder to fly unpredictably, making it challenging to dispense small amounts. A long, beveled metallic needle worked well to transfer PLL-g-PEG. Store PLL-g-PEG powder at –20 °C.

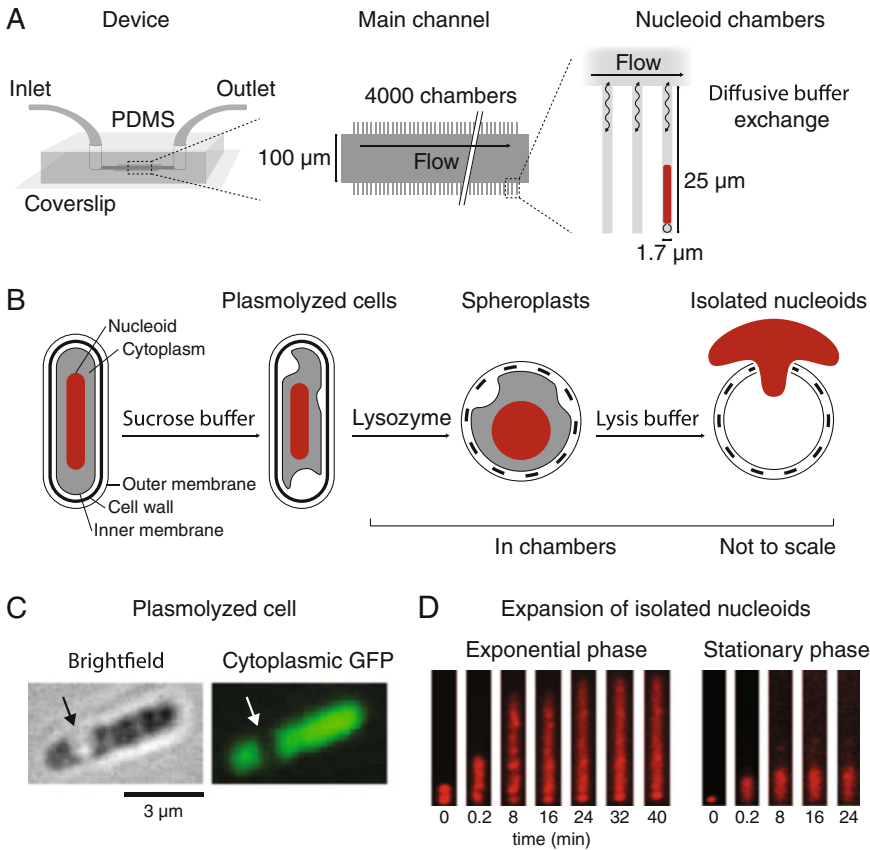


**Fig. 1** Microfluidic lysis procedure. **(a)** The microfluidic device facilitates sequential buffer exchange around cells and isolated nucleoids. A PDMS device bonded to a glass coverslip contains a main channel with thousands of side chambers in which nucleoids are isolated. Diffusion between the channel and chambers enables rapid buffer exchange without subjecting the nucleoids to flow. **(b)** To isolate nucleoids, cells are first plasmolyzed in hypertonic sucrose buffer, relieving turgor pressure on the cell wall. Next, cells are incubated with lysozyme which digests the cell wall, causing cells to lose their rod shape and become more spherical. Last, rapid switch to a hypotonic lysis buffer restores turgor pressure and lyses the vulnerable cell, releasing the nucleoid into the chamber as the cytoplasm diffuses away. **(c)** In plasmolyzed cells, the inner membrane recedes from the cell wall, visible as a region of decreased contrast in brightfield images, and as a region without cytoplasmic GFP fluorescence. **(d)** After lysis, the nucleoid expands rapidly in seconds, then more slowly over tens of minutes. Nucleoid structure varies dramatically with cell physiology, with much larger and more heterogeneous nucleoids from exponential phase cells than stationary phase cells

3.1.2 Device Assembly and Surface Passivation

To prevent nonspecific adsorption of nucleoids, microfluidic surfaces were passivated with 20 kDa poly-L-lysine covalently grafted (grafting ratio 3.5) to 5 kDa polyethylene glycol, PLL(20)-g[3.5]-PEG(5) (SuSoS AG) [7]. We attempted other passivation methods, including bovine serum albumin (BSA), sheared salmon sperm DNA, and *E. coli* lipid extract. In our experience, PLL-g-PEG worked best to reduce nonspecific interactions between nucleoids and microfluidic surfaces. If surface passivation is effective, then nucleoids slide along the chambers in response to osmotic buffer

changes, and nucleoids near the chamber exits may get pulled out of the chambers altogether.

1. Clean glass coverslips.<sup>6</sup>
2. Using a coring tool, core holes through the PDMS device for the inlet and outlet. Core the holes from the surface with channels to the opposite smooth surface, so the holes align with the channels, as shown in Fig. 1.
3. Bond PDMS device to glass coverslip.
4. After bonding, bake device for at least 10 min at 65 °C.
5. Let the device cool to room temperature, then immediately fill the device with 0.1 mg/mL PLL-g-PEG solution in 10 mM Na-HEPES, pH 7.4 (Subheading 2.2).<sup>7</sup>
6. Incubate the device with PLL-g-PEG solution for 30 min at room temperature.
7. Wash the device with sterile water.<sup>8</sup>

## 3.2 Nucleoid Isolation

### 3.2.1 Preparation of Cell Cultures

Nucleoid structure depends on cell physiology, so culture conditions influence nucleoid structure. In any growing culture, cells in different cell cycle stages contain different numbers of chromosome equivalents. In steady state growth, if the chromosome replication time exceeds the doubling time, *E. coli* perform multifork replication. In non-steady state growth, the number of chromosome equivalents per cell may change over time. For example, in LB medium the number of chromosome equivalents decreases from exponential to stationary phase [8]. The distribution of nucleoid structures in the culture is influenced by its history, not just its current optical density. While this protocol uses LB, we also recommend synthetic media and further optimization when physiology is important.

1. The day before the experiment, inoculate cells from an –80 °C glycerol stock into growth medium. We grew cells in 3 mL LB medium at 37 °C in 15 mL polypropylene round bottom tubes, shaken for aeration.
2. Grow the cells to early exponential phase, then dilute the culture at least 1000-fold to increase the number of generations after inoculation.
3. Grow cells to final optical density.

---

<sup>6</sup>We cleaned coverslips with ethanol then deionized water before the ethanol dried. If necessary, use a more elaborate cleaning procedure.

<sup>7</sup>The polycationic PLL associates with hydroxyl moieties generated by plasma treatment of the PDMS and glass surfaces.

<sup>8</sup>When replacing one buffer with another, infuse several times the total volume of the device. It is preferable to use a syringe pump to flow 50 µL at 10 µL/min, though it is possible to gently infuse at a similar rate by hand. We use HPFA+ tubing to infuse all buffers, with the exception of the lysis buffer for which we use the stiffer PEEK tubing (Subheading 2.1).

For exponential phase cells, we grow cultures to OD 0.3.

For stationary phase cells, track the number of hours after an exponential phase OD reference point.

### 3.2.2 Spheroplast Formation

Nucleoid isolation requires effective spheroplast formation, which in turn requires effective plasmolysis. The hypertonic sucrose buffer induces plasmolysis—recession of the inner membrane from the cell wall [9]. At 20% (w/v) (0.58 M) sucrose, cells remain viable [10]. Cells are plasmolyzed outside the device then loaded into microfluidic chambers. Spheroplasts are more delicate than plasmolyzed cells, so they are formed in the chambers rather than flowed into the device. Lysozyme treatment digests the peptidoglycan cell wall, making the cells susceptible to osmotic pressure changes, causing cells to rupture in hypotonic solution.

1. Centrifuge 750  $\mu\text{L}$  cell culture in a 1.5 mL tube for 1 min at  $16 \times 10^3$  rcf.<sup>9</sup>
2. Remove as much supernatant as possible, using a 200  $\mu\text{L}$  pipette tip.
3. Resuspend cells in 750  $\mu\text{L}$  sucrose buffer (Subheading 2.2), pipetting gently to disperse the pellet. Do not vortex.
4. Leave plasmolyzed cells gently rotating on a rotisserie at room temperature until loading them to a passivated microfluidic device, no more than 1 h after resuspending them in sucrose buffer.
5. Flow sucrose buffer into the microfluidic device, to displace water after PLL-g-PEG surface treatment.
6. Prepare a 10 mg/mL lysozyme stock solution in sterile water. Keep on ice and use on the same day. Prepare 300  $\mu\text{g}/\text{mL}$  lysozyme in sucrose buffer.
7. Centrifuge plasmolyzed cells for 1 min at  $16 \times 10^3$  rcf, then resuspend in 100  $\mu\text{L}$  sucrose buffer without lysozyme.
8. Flow plasmolyzed cells into the device.
9. Load cells into chambers. Depending on the experiment, we aimed for one or two cells per chamber.

Option 1. Allow cells to drift into chambers, which works well for concentrated stationary phase cells. PDMS is permeable to water [11], and the permeation flux helps load cells into the chambers.

Option 2. Spin the entire device using a small microcentrifuge, which helps load larger exponential phase cells into

<sup>9</sup> Depending on the optical density of the culture, the volume of the microfluidic device, and the strategy to load cells into chambers (step 9), scale the volume up or down.

chambers, by increasing the concentration of cells near the chamber entrances.

10. Wait for several minutes for cells to drift to the chamber ends.
11. Flow lysozyme in sucrose buffer into the device.
12. Incubate cells in lysozyme for 30 min at 30 °C.

### 3.2.3 Cell Lysis and Nucleoid Isolation

After lysozyme treatment, hypotonic buffer lyses vulnerable spheroplasts, releasing nucleoids into the chamber. After lysis, the cytoplasm diffuses out of the chamber, but the cell envelope remains in the chamber. Lysis buffer should be infused as fast as possible, to thoroughly remove lysozyme at the moment of lysis, as lysozyme is cationic and can compact DNA.

As the salt concentration in the lysis buffer increased, the synchronization of lysis decreased. At 100 mM NaCl, almost all cells lysed at the moment lysis buffer arrived. At 150 mM NaCl, many cells lysed minutes after lysis buffer arrived. At 200 mM NaCl, the highest salt concentration studied, we observed little to no lysis. Salts increase the osmotic pressure and thus decrease the osmotic shock. Furthermore, monovalent ions increase membrane stability by screening electrostatic repulsion between lipids, whereas multivalent ions dramatically increase membrane stability [12].

1. Fill PEEK tubing with lysis buffer (Subheading 2.2).
2. Arrange the tubing so it does not torque the microfluidic device.<sup>10</sup>
3. Make sure the flow is stopped completely.<sup>11</sup>
4. Press tubing into inlet, leaving about 0.5 µL dead volume in the inlet.
5. Mount the device on the microscope.<sup>12</sup>
6. To image nucleoid expansion after lysis, start acquisition before starting the flow of lysis buffer.<sup>13</sup>
7. Start the flow of lysis buffer at 2000 µL/h.
8. After lysis, continue to flow lysis buffer at 50 µL/h, for the duration of the experiment.<sup>14</sup>

---

<sup>10</sup> Tape the tubing to the stage, so that the device and tubing move together as a firm unit when the stage moves. Add a short 90° bend just above the device inlet, so that the tubing is not pushed by the condenser lens.

<sup>11</sup> Otherwise, spheroplasts may lyse before the start of image acquisition. A pressure-driven pump or hydrostatic pressure system [6] offers precise control of flow.

<sup>12</sup> To prevent motion of the device during the experiment, adhering the device with double-sided tape to a stage insert works well.

<sup>13</sup> At 100 mM NaCl, lysis is nearly instantaneous upon arrival of lysis buffer. Since nucleoid expansion after lysis is rapid, per experiment we often follow just one field of view containing about ten nucleoids. At higher salt concentrations, such as 150 mM NaCl, many cells lyse minutes after infusion of lysis buffer.

<sup>14</sup> This helps to maintain a constant biochemical environment, for example to wash dissociated proteins from the device.

### 3.3 Imaging

#### 3.3.1 Microscopy

We imaged nucleoids and cells on an inverted microscope (Nikon Eclipse Ti-E) with a high numerical aperture 100× objective lens (Nikon CFI Apo TIRF 100× oil). To minimize photodamage and photobleaching, we imaged with an EM-CCD (Hamamatsu ImageEM C9100-13) with minimal illumination, using the ND32 neutral density filter on the lamp (Nikon Intensilight C-HGFI). We used widefield epifluorescence to image nucleoids, and differential interference contrast (DIC) to image the cell envelope after lysis. To image dynamics at short and long time scales, we acquired images in two phases.

1. For the first minute, we image at 20 frames per second, with the shutter open continuously, to image rapid expansion of the nucleoid at the moment of lysis.
2. For the rest of the experiment, we image at 5 s per frame, with the shutter closed between frames, to minimize exposure while imaging slow continued expansion and structural relaxation of the nucleoid.

#### 3.3.2 Fluorescent Probes

As a native marker of the whole nucleoid, we used the nucleoid-associated protein HU fused to a fluorescent protein [13]. HU is highly abundant, with on the order of  $10^4$  copies per cell, and it exhibits low sequence specificity [14, 15]. HU is a dimer, composed of  $\alpha$  or  $\beta$  subunits, encoded by the genes *hupA* or *hupB*, respectively. HU influences nucleoid structure, so to express the HU fluorescent fusion at natural levels, we used a strain with *hupA* replaced by *hupA-mCherry* or *hupA-GFP* at its native chromosomal locus [16, 17]. The fluorescent fusion was functional, as deletion of *hupB* did not cause cellular filamentation, characteristic of double mutants lacking both *hupA* and *hupB* [18].

DNA dyes, such as Hoechst 33342 (Subheading 2.2), are another nucleoid labeling option. Hoechst permeates cells, so before resuspending cells in sucrose buffer, add 10  $\mu\text{g}/\text{mL}$  Hoechst to the growth medium and incubate for 20 min at room temperature. Alternatively, Hoechst may be included in the lysis buffer to label nucleoids after isolation. Hoechst permeates the PDMS, increasing the background fluorescence, but the signal from nucleoids was often high enough to discern the nucleoids over the background.

### 3.4 Biochemical Characterization of Nucleoid-Associated Proteins

Microfluidic nucleoid isolation enables biochemical characterization of nucleoid-associated proteins (NAPs), such as measurement of their unbound fractions and off-rates. During the *in vivo* to *in vitro* transition, the whole nucleoids start with a full complement of NAPs at *in vivo* concentrations. After lysis, NAPs dissociate from nucleoids and escape from the chambers.

Isolate nucleoids as described in Subheading 3.2, then measure the total mCherry intensity to estimate the amount of



HU-mCherry remaining on the nucleoid. To estimate photobleaching, we measured the fluorescence decrease in unlysed cells. During the first acquisition phase, with the shutter open continuously, photobleaching was significant, with an exponential decay constant of about 2 min. During the second phase, with the shutter closed between frames, photobleaching was negligible.

### 3.4.1 Measurement of Unbound Fraction

After lysis, cytoplasmic proteins not associated with the nucleoid, including transiently unbound NAPs, diffuse from the microfluidic chambers. At the moment of lysis, the total HU-mCherry intensity abruptly decreased several percent (Fig. 2), which we identify as the fraction of HU not initially bound to the nucleoid.

The maximum fractional drop  $I_{\text{HU}}(t + 50 \text{ ms})/I_{\text{HU}}(t)$  between subsequent 50 ms time points estimates a lower limit on the fraction of unbound HU-mCherry. This metric underestimates the unbound fraction, as some HU-mCherry may not escape within the first 50 ms after lysis, and some HU-mCherry remains trapped in the cell envelope after lysis.

### 3.4.2 Measurement of Off-Rate

After nucleoid isolation, the device enables measurement of the off-rate versus time. Soon after lysis, trajectories exhibited nonexponential decay, perhaps due to a range of binding site affinities (Fig. 2). For example, HU has a higher affinity for kinked, cruciform, and nicked DNA structures [19–21]. At later times, the trajectories converged to exponential decay. We estimated a lower limit on the off-rate based on the exponential regime. The half-life

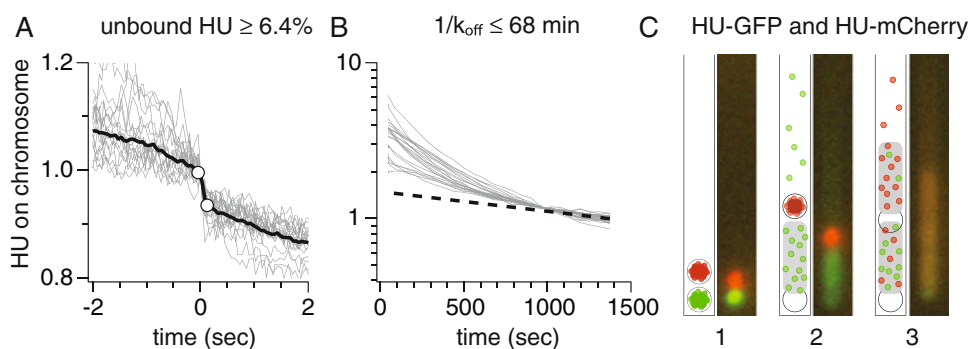


**Fig. 2** Biochemical characterization of HU-mCherry by monitoring its dissociation from isolated nucleoids. (a) At the moment of lysis, the integrated HU-mCherry fluorescence abruptly drops a few percent, which we attribute to the rapid escape of cytoplasmic HU-mCherry not initially bound to the nucleoid. Cytoplasmic fluorescent proteins diffuse away abruptly after lysis (data unpublished). *Gray traces* represent individual trajectories, and the *black trace* represents the average trajectory. (b) HU-mCherry exhibits nonexponential decay at short times and approaches exponential decay at long times. Fitting the latter regime provides a lower bound on the off-rate. (c) HU redistributes across different nucleoids in the same chamber. The cell containing HU-GFP lyses first. After the cell containing HU-mCherry lyses, some HU-mCherry binds to the HU-GFP nucleoid and vice versa

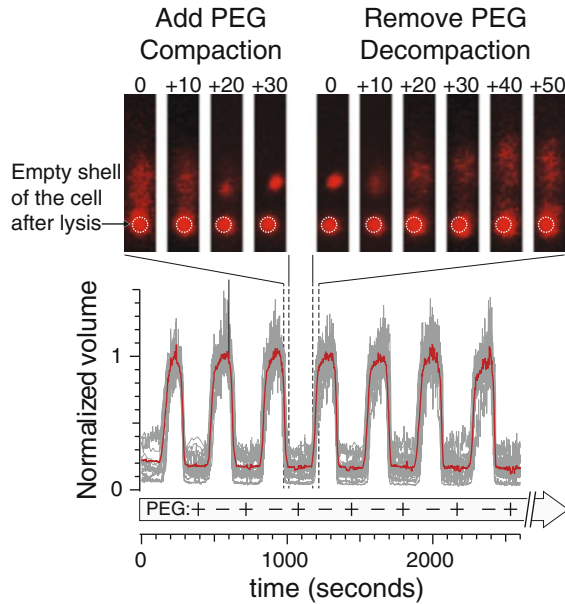


**Fig. 3** Molecular crowding of isolated nucleoids. After nucleoid isolation, we oscillated the concentration of 20 kDa polyethylene glycol (PEG) in the ambient buffer. At 29% (w/v) PEG, nucleoids were abruptly compacted to in vivo size. At 3% (w/v) PEG, nucleoids expanded again, with dynamics comparable to expansion after lysis. Nucleoid compaction and decompaction was reversible and repeatable for many cycles

is a useful approximation for how long NAPs are bound to the nucleoid.

We measured dependence of the off-rate on the ambient salt concentration, between 40 and 200 mM NaCl. Below 40 mM NaCl, viscous drag pulled the longer exponential phase nucleoids out of the chambers. Above 200 mM NaCl, few to no cells lysed. HU-mCherry dissociated faster at higher salt concentrations. At each salt concentration, HU-mCherry dissociated faster from stationary phase nucleoids than from exponential phase nucleoids.

The dissociation rate of bound HU may also depend on the ambient NAP concentration [22, 23]. To test unbinding and rebinding of NAPs, we lysed strains containing HU-GFP and HU-mCherry in the same chamber, and we observed redistribution of the proteins across nucleoids (Fig. 3).

### 3.5 Osmotic Compression of Nucleoids

The microfluidic device enables biochemical perturbation of isolated nucleoids. For example, we exposed isolated nucleoids to different polyethylene glycol (PEG) solutions, to study the effects of molecular crowding on nucleoid structure.

For fast and precise control of the ambient buffer, we used a multiport valve (Subheading 2.1) to switch between solutions with 3% (w/v) or 29% (w/v) PEG, each controlled by its own syringe pump. We used LabVIEW software to coordinate switching the valve with changing the syringe pump infuse rates. Alternatively,

use a microfluidic mixer, a module that merges and mixes streams from the different syringe pumps. In principle, a mixer can interpolate between the high and low concentrations, based on the relative infuse rates. In practice, make sure that the module sufficiently mixes the laminar streams, and characterize the transients after changing infuse rates. To decrease the delay after buffer change, minimize the length of tubing between the valve and device.

---

## Acknowledgments

J.F.P. was supported by a Fannie and John Hertz Graduate Fellowship, and S.J. by Paul G. Allen Foundation, Pew Charitable Trusts, NSF CAREER, and NIH GM118565-01.

## References

1. Dillon SC, Dorman CJ (2010) Bacterial nucleoid-associated proteins, nucleoid structure and gene expression. *Nat Rev Microbiol* 8(3):185–195
2. Stavans J, Oppenheim A (2006) DNA-protein interactions and bacterial chromosome architecture. *Phys Biol* 3:R1
3. Ali Azam T, Iwata A, Nishimura A, Ueda S, Ishihama A (1999) Growth phase-dependent variation in protein composition of the *Escherichia coli* nucleoid. *J Bacteriol* 20:6361
4. Pelletier J, Halvorsen K, Ha B-Y, Paparcone R, Sandler SJ, Woldringh CL, Wong WP, Jun S (2012) Physical manipulation of the *Escherichia coli* chromosome reveals its soft nature. *Proc Natl Acad Sci U S A* 109:E2649–E2656
5. Cunha S, Odijk T, Süleymanoglu E, Woldringh CL (2001) Isolation of the *Escherichia coli* nucleoid. *Biochimie* 83:149–154
6. Amir A, Babaepour F, McIntosh DB, Nelson DR, Jun S (2014) Bending forces plastically deform growing bacterial cell walls. *Proc Natl Acad Sci U S A* 111:5778–5783
7. Lee S, Vörös J (2005) An aqueous-based surface modification of poly(dimethylsiloxane) with poly(ethylene glycol) to prevent biofouling. *Langmuir* 21:11957–11962
8. Akerlund T, Nordstrom K, Bernander R (1995) Analysis of cell size and DNA content in exponentially growing and stationary-phase batch cultures of *Escherichia coli*. *J Bacteriol* 177:6791–6797
9. Rojas E, Theriot JA, Huang KC (2014) Response of *Escherichia coli* growth rate to osmotic shock. *Proc Natl Acad Sci U S A* 111:7807–7812
10. Pilizota T, Shaevitz JW (2014) Origins of *Escherichia coli* growth rate and cell shape changes at high external osmolality. *Biophys J* 107:1962–1969
11. Randall GC, Doyle PS (2005) Permeation-driven flow in poly(dimethylsiloxane) microfluidic devices. *Proc Natl Acad Sci U S A* 102:10813–10818
12. Ha B-Y (2001) Stabilization and destabilization of cell membranes by multivalent ions. *Phys Rev E* 64:051902
13. Wery M, Woldringh CL, Rouviere-Yaniv J (2001) HU-GFP and DAPI colocalize on the *Escherichia coli* nucleoid. *Biochimie* 83:193–200
14. Ali Azam T, Hiraga S, Ishihama A (2000) Two types of localization of the DNA-binding proteins within the *Escherichia coli* nucleoid. *Genes Cells* 5:613–626
15. Krylov AS, Zasedateleva OA, Prokopenko DV, Rouviere-Yaniv J, Mirzabekov AD (2001) Massive parallel analysis of the binding specificity of histone-like protein HU to single- and double-stranded DNA with generic oligodeoxyribonucleotide microchips. *Nucleic Acids Res* 29(12):2654–2660
16. Centore RC, Lestini R, Sandler SJ (2008) XthA (Exonuclease III) regulates loading of RecA onto DNA substrates in log phase *Escherichia coli* cells. *Mol Microbiol* 67:88–101
17. Marceau AH, Bahng S, Massoni SC, George NP, Sandler SJ, Mariani KJ, Keck JL (2011) Structure of the SSB-DNA polymerase III interface and its role in DNA replication. *EMBO J* 30:4236–4247
18. Dri AM, Rouviere-Yaniv J, Moreau PL (1991) Inhibition of cell division in hupA hupB mutant bacteria lacking HU protein. *J Bacteriol* 173:2852–2863

19. Pontiggia A, Negri A, Beltrame M, Bianchi ME (1993) Protein HU binds specifically to kinked DNA. *Mol Microbiol* 7:343–350
20. Kamashev D, Balandina A, Rouviere-Yaniv J (1999) The binding motif recognized by HU on both nicked and cruciform DNA. *EMBO J* 18:5434–5444
21. Kamashev D, Rouviere-Yaniv J (2000) The histone-like protein HU binds specifically to DNA recombination and repair intermediates. *EMBO J* 19:6527–6535
22. Graham JS, Johnson RC, Marko JF (2011) Concentration-dependent exchange accelerates turnover of proteins bound to double-stranded DNA. *Nucleic Acids Res* 39:2249–2259
23. Hadizadeha N, Johnson RC, Marko JF (2016) Facilitated dissociation of a nucleoid protein from the bacterial chromosome. *J Bacteriol* 198:1735–1742